Generation and Complete Electric-Field Characterization of Intense Ultrashort Tunable Far-Infrared Laser Pulses

G. M. H. Knippels,[1,*] X. Yan,[2] A. M. MacLeod,[2] W. A. Gillespie,[2] M. Yasumoto,[3]
D. Oepts,[1] and A. F. G. van der Meer[1]
[1]FOM-Institute for Plasma Physics "Rijnhuizen," P.O. Box 1207, 3430 BE, Nieuwegein, The Netherlands
[2]School of Science and Engineering, University of Abertay Dundee, Bell Street, Dundee DD1 1HG, United Kingdom
[3]Osaka National Research Institute, AIST (ONRI), 1-8-31 Midorigaoka, Ikeda Osaka 563-8577, Japan
(Received 1 March 1999)

Intense rapidly tunable picosecond laser pulses have been generated in the far infrared from 30 to 250 μm, a range not well covered by other sources. The transform-limited, diffraction-limited pulses have energies of up to 17 μJ, peak powers of more than 1 MW, a length of only 18 optical periods, and focused intensities of 0.1 GW/cm^2. Measurements of both the optical field amplitude and the phase have been performed at 150 μm with a rapid-scanning cross-correlation technique probing the field-induced birefringence in ZnTe with a 10-fs Ti:sapphire laser. The far-infrared laser opens up the exciting possibility of performing nonlinear experiments in a relatively unexplored spectral range.

PACS numbers: 41.60.Cr

Free-electron lasers (FELs) are well established as a versatile source of high-intensity rapidly tunable laser radiation in wavelength ranges where other laser sources are scarce. In particular, the mid- to far-infrared part of the spectrum (3–1000 μm) can conveniently be covered by FELs because of the rather modest requirements on the accelerator that provides the electron beam. This has led to the development of several international infrared FEL facilities which serve a broad range of scientific users [1]. FELs produce high pulse energies in transform-limited pulses of variable bandwidth, in strong contrast to the weak broadband terahertz (THz) radiation sources [2] that are pumped by Ti:sapphire (Ti:S) femtosecond laser systems.

A key feature of the new FEL, constructed at the Free-Electron Laser for Infrared Experiments Facility (FELIX) [3], is that it operates at long wavelengths (30–250 μm) with short electron pulses (0.3-mm rms).

A characteristic parameter is the longitudinal decoupling parameter μ_c, which is the ratio between the slippage distance L_s ($L_s = N\lambda$, where N is the number of undulator periods and λ is the laser wavelength) and the (rms) electron bunch length σ_e. In our case, μ_c ranges from 4 to 30, while the largest value used in other FELs is $\mu_c \approx 2.2$. The slippage distance is the difference between the distances traveled by an electron and an optical wave front, respectively, during the electron's transit through the undulator. It is also the range over which transients due to the electron pulse edges influence the optical pulse. The operation of a short-pulse, large-slippage FEL oscillator is sensitive to the synchronism between the optical pulses circulating in the laser cavity and the injected electron pulses. The cavity detuning ΔL, i.e., the difference between the actual cavity length and the synchronous length for which the round-trip time of the optical wave exactly matches the electron repetition interval, is an important parameter in the FEL interaction dynamics. The formation of the optical pulses in a FEL with large μ_c is a delicate balance between desynchronism, gain, and saturation. It is possible to generate optical pulses that are much shorter than L_s and therefore contain only a few cycles of the optical field. The laser behavior at short optical pulse lengths and high intracavity powers has been demonstrated to scale according to super-radiant scaling laws [4], related to the "spiking" mode of operation that is observed for values of μ_c smaller than unity [5].

The design of the large-slippage free-electron laser has been reported elsewhere [6]. A one-dimensional waveguide is used to reduce the diffraction losses at long wavelengths. Some machine parameters are summarized in Table I. This Letter describes the characterization of the optical output of the newly built FEL, such as small-signal gain, cavity losses, pulse energy, and beam quality, and focuses on the complete characterization of the electric field amplitude and phase of the picosecond FEL infrared (IR) pulses.

Characterization of the laser output.—In Fig. 1(a) the measured pulse energy is shown as a function of the laser wavelength. The picosecond pulses (micropulses) arrive in a burst 5–10 μs long (macropulse) with a micropulse spacing of 1 ns (1 GHz repetition rate). The macropulses are repeated at 10 Hz, leading to an average power of a few hundred milliwatts. Typically, 50%–70% of the measured pulse energy is available for experiments since

TABLE I. Parameters for the long-wavelength FELIX laser.

Electron energy	12–25 MeV
Peak current	50 A
Undulator period	65 mm
Number of periods	38
Normalized vector potential	1.9 (rms, max)
Optical cavity length	6 m
Waveguide width	10 mm

 0031-9007/99/83(8)/1578(4)$15.00

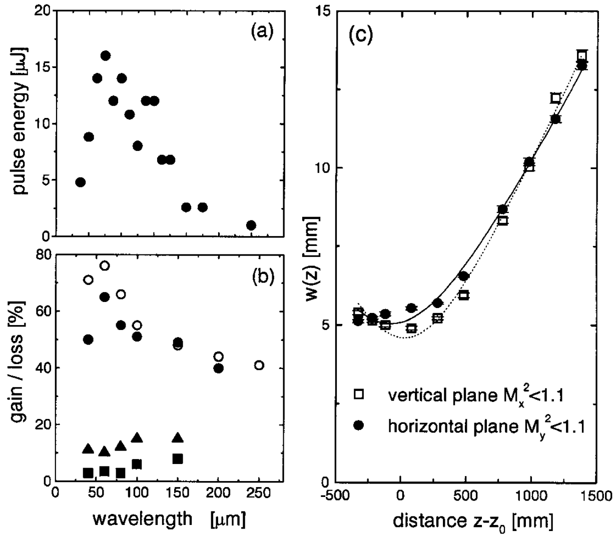

FIG. 1. The measured optical pulse energy versus wavelength at the outcoupler is shown in (a). The measured gross gain (solid dots) and calculated gain [6] (open dots) are shown in (b). The triangles are the measured cavity round-trip loss, whereas the squares correspond to the estimated contribution of the out-coupling to the round-trip loss. (c) The Gaussian spot size variation at 150-μm wavelength when the laser beam is weakly focused for both the horizontal (solid dots) and vertical plane (open squares). The fits (solid line for the horizontal plane and dotted line for the vertical plane) indicate a diffraction-limited beam.

the beam has to be transported through an evacuated transport system containing up to 30 metal mirrors to the user area. In Fig. 1(b) the measured gross gain (solid dots) is plotted together with the calculated [6] gross gain (open dots) and is seen to agree fairly well. The solid triangles in Fig. 1(b) represent the measured round-trip loss, whereas the estimated round-tip loss due to out-coupling through the hole in one of the end mirrors is indicated by a solid square. The round-trip loss is calculated from an exponential fit to the ring-down at the end of the macropulse. For a reason that is not yet well understood the cavity loss increases more rapidly with wavelength than anticipated from calculations (no data points are given at longer wavelengths since the detector employed was not fast enough to measure cavity losses in excess of 16%). This is probably the cause of the rapid drop in the out-coupled pulse energy above 120 μm. Transverse beam size measurements have been performed [see Fig. 1(c)] at 150-μm wavelength with a 2 × 2 in. pyroelectric array (LBA200, Spiricon). All measurements yield a clean symmetric beam profile and show diffraction-limited beam quality ($M^2 < 1.1$) [7].

To study the optical pulse duration and shape we adapted a cross-correlation technique frequently used to characterize other THz sources [8]. The technique probes the electric-field-induced birefringence in a linear electro-optic (EO) crystal with a laser at visible (or near-infrared) frequencies. ZnTe is an ideal EO crystal because of its good optical properties at the probing Ti:S frequency as well as at THz frequencies. The setup used in our experiment is shown schematically in Fig. 2(a). A Si photodiode measures the intensity of the Ti:S radiation, which passes through a pair of crossed polarizers placed around the 500-μm-thick ZnTe crystal (Uni-export, U.K.). The Ti:S laser, producing 3-nJ, 10-fs pulses at 100 MHz repetition rate (Femto Source Pro, Femto Lasers, Vienna), is actively synchronized to the FEL optical output, and the total jitter between the two lasers is approximately 1 ps FWHM over a time scale of several minutes [9]. (Note that the Ti:S laser operates at 100 MHz and samples four independent FEL pulses circulating in the 6-m-long cavity. In total, 40 pulses are present in the cavity since the FEL electron bunches arrive at 1 GHz rate.) The Ti:S pulse train enters the EO crystal with its direction of polarization rotated by 45° with respect to the polarization direction of the incident FEL pulse; the FEL-induced birefringence causes a phase difference between the components parallel and perpendicular to the direction of the FEL polarization. This acquired phase difference is proportional to the FEL's electric-field strength in the crystal and causes the Ti:S radiation to become elliptically polarized and to pass partly through the second polarizer. For small phase retardation the intensity of the Ti:S radiation emerging from the second polarizer is proportional to the square of the electric field, i.e., the intensity of the FEL pulse, and this has been verified by power dependence measurements. The intensity profile can be measured, with a temporal resolution given by the jitter of 1 ps, by varying the optical delay between the Ti:S pulse and the FEL micropulse.

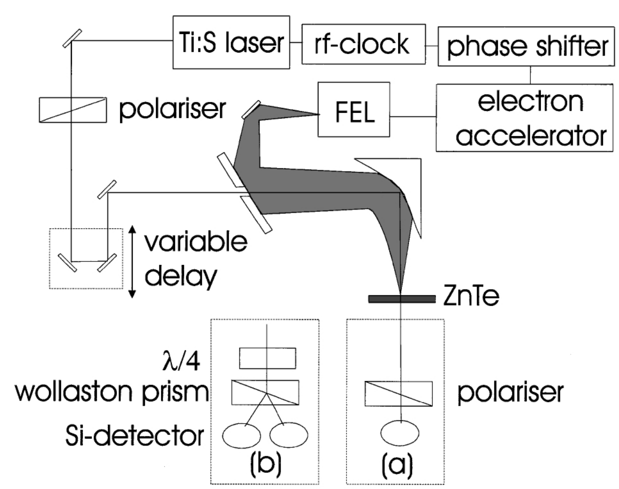

FIG. 2. The EO cross-correlation setup with two different detectors (a) and (b). In (a) the measured photodiode intensity is proportional to the FEL intensity. In (b) the measured photodiode intensity is proportional to the instantaneous electric field strength of the FEL pulse.

Figure 3 shows a series of EO measurements and power spectra (see insets) of the FEL micropulses at 150 μm wavelength and with cavity detunings ΔL of (a) -100 μm, (b) -300 μm, and (c) -600 μm. These measurements demonstrate that the FEL pulse length and shape are strongly influenced by the value of ΔL, and for large values of ΔL the optical pulse develops a leading edge that can be fitted well with an exponential [10]. Calculation of the time-bandwidth product for different cavity detunings gives values in the range of 0.2–0.3 when the pulse has a clear exponential tail, e.g., Figs. 3(b) and 3(c). In the case of Fig. 3(a) the optical pulse shape is closer to a Gaussian and the time-bandwidth product is 0.6.

It is well known [8] that a more sensitive measurement of the EO effect can be performed if the second polarizer is replaced by the combination of a $\frac{1}{4}\lambda$ wave plate and a polarizing beam splitter as shown in Fig. 2(b). Both Ti:S polarization components can then be detected on two separate Si diodes, and the $\frac{1}{4}\lambda$ wave plate provides an optical bias so that the response of each diode for small phase retardation is now proportional to the electric-field strength instead of the intensity. A typical measurement, where the signal from one macropulse of the FEL is taken at a fixed setting of the delay line, is shown in Fig. 4(a). The jitter between the Ti:S laser and the FEL is negligibly small on this fast time scale and consequently we are dealing with two perfectly synchronized laser systems [11]. The Ti:S repetition frequency is phase locked to the electron bunch repetition frequency, and therefore also to the FEL pulse envelope round-trip frequency (the FEL gain keeps the pulse envelope at the position of the electron bunches). This means that, during the macropulse, the Ti:S pulse train samples the envelope of the circulating FEL micropulses at the same position. However, the phase of the FEL carrier wave shifts in each round-trip with respect to the envelope by $\Delta\phi_{\text{rel}} = 2\pi \times 2\Delta L/\lambda$, depending on the applied cavity detuning. This relative phase shift leads to the beat signal observed in Fig. 4(a), with frequency f_{beat},

$$f_{\text{beat}} = \frac{-2\Delta L}{\lambda}\frac{c}{2L}\,.$$

Here L is the length of the cavity (6 m).

When $\Delta L = k \times \lambda/2$ with integer k, the phase advance per round-trip is just $k \times 2\pi$, and is indistinguishable from zero, and so the observed beat frequency is actually $f_{\text{beat}}\,\text{mod}(c/2L)$. The values of $\Delta L_k = k \times \lambda/2$ at which the observed beat frequency is zero, can be determined with an accuracy of about 0.5 μm, or a few parts in a thousand of the laser wavelength. In a dispersionless cavity there is one exact synchronism position ($k = 0$). This position can be found by varying the wavelength, as ΔL_k is independent of λ only when $k = 0$. In our present

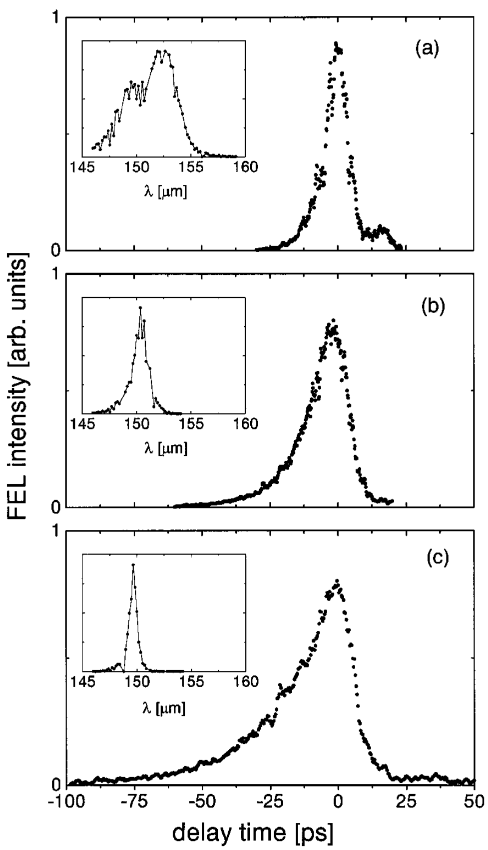

FIG. 3. Measured optical pulse shapes (a)–(c), using the EO cross-correlation technique described in the text, and power spectra (insets) at 150-μm wavelength for ΔL of -100 μm (a), -300 μm (b), and -600 μm (c). The leading edge of the optical pulse (negative delay times) is exponential for large values of ΔL [10]. The time-bandwidth products are 0.59, 0.20, and 0.22 in (a)–(c), respectively.

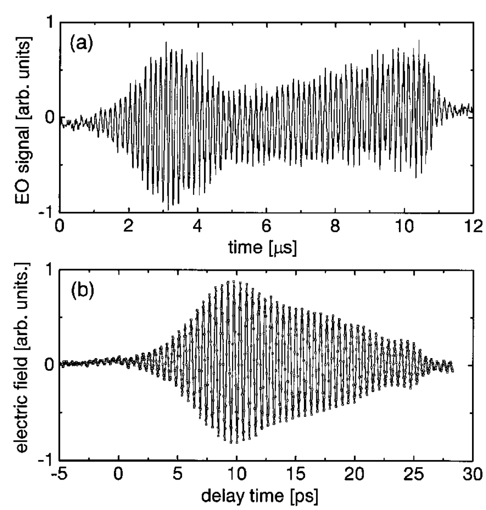

FIG. 4. EO signal recorded during a macropulse with $\Delta L = -20$ μm (a). The beat signal results from a phase shift per round-trip of $2\pi \times 2\Delta L/\lambda$ of the FEL carrier wave with respect to the Ti:S pulse train, causing the Ti:S pulses to sample different phases of the electric-field cycles. In (b) the micropulse electric-field profile of the FEL pulse is shown (see text for details).

case, the waveguide introduces noticeable dispersion, and the group velocity synchronism differs from the phase velocity synchronism. Taking this into account, it is still possible to determine the exact cavity length with high precision.

The ability to measure the details of the electric field with this EO detection method opens up the possibility of measuring the complete FEL pulse envelope profile, including the individual electric-field cycles, thereby completely characterizing the optical output. The fact that the jitter between the Ti:S pulse train and the FEL pulse train is extremely small during a macropulse also allows a high-temporal resolution measurement, provided that the delay between the Ti:S pulse and the FEL pulse can be scanned far enough during these few microseconds. This can be achieved by operating the FEL at a slightly different frequency than the Ti:S laser, so that the pulse trains sweep over each other. In view of the low duty factor of the FEL it is necessary to start this different frequency just before the FEL macropulse arrives. This can be done by switching the frequency of the rf clock driving the accelerating structures of the FEL with a voltage-controlled rf-phase shifter (and switching it back after the macropulse has passed). The FEL cavity length has to be set such that the cavity detuning has the correct value for the shifted rf-clock frequency. The frequency-switching technique has already been demonstrated in the past as a way of obtaining short and stable optical pulses [12], and is now adapted to rapidly scan the delay between the Ti:S laser pulses and the envelope and carrier wave of the FEL pulse.

Figure 4(b) shows a measurement of the electric-field profile of a micropulse using this rapid-scanning technique. A frequency offset of 3 ppm is applied just before the beginning of the macropulse. This results in a speed of 0.133 ps/round-trip, equivalent to 3.3 ps/μs, at which the Ti:S pulse train and the FEL pulse train sweep over each other. Provided that the effective FEL cavity detuning is equal to $k\lambda/2$, and undersampling in the data acquisition is avoided, the observed beat signal corresponds to the FEL electric-field cycles. Therefore, Fig. 4(b) is the electric-field profile of the FEL micropulse. Since the technqiue acquires the trace within one macropulse, it is only a relevant measurement if the micropulse shape does not change significantly during the macropulse. We have indications that this condition is sufficiently well fulfilled in our case. The observed number of cycles at the FWHM is 26, corresponding to only 18 optical cycles FWHM of the intensity profile.

In conclusion, we have generated intense picosecond far-infrared laser pulses from 30 to 250 μm in a waveguide free-electron laser. The shortest pulses observed at 150 μm have a length of only 18 optical field cycles at the FWHM of the intensity profile. The combination of short pulse duration, high pulse energy, and diffraction-limited beam quality leads to unprecedented power densities of up to 0.1 GW/cm^2, allowing nonlinear experiments in a wide range of the far-infrared spectrum. The electric-field profile of the optical pulses has been characterized with a rapid-scanning cross-correlation technique with an actively synchronized 10-fs Ti:S laser. This technique allows complete characterization of the optical output as well as accurate experimental determination of one of the most important parameters for free-electron lasers, the absolute cavity detuning.

We thank Dr. C. W. Rella and Dr. P. C. M. Planken for valuable discussions. This work is part of the research program of the "Stichting voor Fundamenteel Onderzoek der Materie (FOM)," which is financially supported by the "Nederlandse Organisatie voor Wetenschappelijk Onderzoek" (NWO). X. Y., A. M. M., and W. A. G. are grateful to the UK Engineering and Physical Sciences Research Council for financial support (Grant Code No. GR/M13602). M. Yasumoto is grateful to the Japanese Science and Technology Agency for financial support.

*Corresponding author: FOM-Institute for Plasma Physics, P.O. Box 1207, 3430 BE, Nieuwegein, The Netherlands. Email address: knippels@rijnh.nl

[1] G. Ramian, Nucl. Instrum. Methods Phys. Res., Sect. A **318**, 225 (1992); T. I. Smith *et al.*, Nucl. Instrum. Methods Phys. Res., Sect. A **304**, 812 (1992); R. Prazeres *et al.*, Nucl. Instrum. Methods Phys. Res., Sect. A **358**, 212 (1995); F. Ciocci *et al.*, Phys. Rev. Lett. **70**, 928 (1993); T. Tomimasu *et al.*, Nucl. Instrum. Methods Phys. Res., Sect. B **144**, 1 (1998).
[2] D. You *et al.*, Opt. Lett. **18**, 290 (1998).
[3] D. Oepts *et al.*, Infrared Phys. Technol. **36**, 297 (1995).
[4] D. A. Jaroszynski *et al.*, Phys. Rev. Lett. **78**, 1699 (1997).
[5] R. W. Warren *et al.*, Nucl. Instrum. Methods Phys. Res., Sect. A **250**, 19 (1986).
[6] L. Lin *et al.*, Rev. Sci. Instrum. **68**, 4342 (1997).
[7] A. E. Siegman, Proc. SPIE Int. Soc. Opt. Eng. **1224**, 2 (1990).
[8] J. A. Valdmanis *et al.*, Appl. Phys. Lett. **41**, 211 (1982).
[9] G. M. H. Knippels *et al.*, Opt. Lett. **23**, 1754 (1998).
[10] This has been measured previously at the Stanford facility at a much shorter FEL wavelength of 6.3 μm; see C. W. Rella *et al.*, Opt. Commun. **157**, 335 (1998).
[11] A. Poppe *et al.*, IEEE J. Quantum Electron. **4**, 179 (1998).
[12] R. J. Bakker *et al.*, Phys. Rev. E **48**, R3256 (1993).